

Phase-Space Structure & Substructure of Dark Halos

Avishai Dekel

Racah Inst. of Physics, The Hebrew University, Jerusalem 91904, Israel

Itai Arad

Institute of Astronomy, Madingley Road, Cambridge CB3 0HA, UK

Abstract. A method is presented for computing the 6-D phase-space density $f(\mathbf{x}, \mathbf{v})$ and its PDF $v(f)$ in an N-body system. It is based on Delaunay tessellation, yielding $v(f)$ with a fixed smoothing window over a wide f range, independent of the sampling resolution. It is found that in a gravitationally relaxed halo built by hierarchical clustering, $v(f)$ is a robust power law, $v(f) \propto f^{-2.5 \pm 0.05}$, over more than 4 decades in f , from its virial level to the current resolution limit. This is valid for halos of different sizes in the Λ CDM cosmology, indicating insensitivity to the initial-fluctuation power spectrum as long as the small-scale fluctuations were not completely suppressed. By mapping f in position space, we find that the high- f contributions to $v(f)$ come from the “cold” subhalos within the parent halo rather than the halo central region and its global spherical profile. The f in subhalos near the halo virial radius is more than 100 times higher than at the halo center, and it decreases gradually with decreasing radius. This indicates phase mixing due to mergers and tidal effects involving puffing up and heating. The phase-space structure provides a sensitive tool for studying the evolution of subhalos during the buildup of halos. One wishes to understand why the substructure adds up to the universal power law in $v(f)$. It seems that the $f^{-2.5}$ behavior is related to the hierarchical clustering process and is not a general result of violent relaxation.

1. Introduction

Dark-matter halos are the basic entities in which luminous galaxies form and live. They dominate the gravitational potential and have a crucial role in determining the galaxy properties. While many of the systematic features of halo structure and kinematics have been revealed by N -body simulations, the origin of these features is still not understood, despite the fact that they are governed by simple Newtonian gravity.

The halo density profile $\rho(r)$ is a typical example. It is found in the simulations to have a robust non-power-law shape (originally Navarro, Frenk & White 1997, NFW; Power et al. 2003; Hayashi et al. 2004 and references therein), with a log slope of -3 at large radii, varying gradually toward -1 or even flatter at

small radii. The slope shows only a weak sensitivity to the cosmological model and the initial fluctuation power spectrum (e.g. Colin et al. 2003; Navarro et al. 2004), indicating that its origin is due to a robust relaxation process rather than specific initial conditions. In particular, violent relaxation (Lynden-Bell 1967) may be involved in shaping up the density profile, but we have no idea why this profile has the specific NFW shape.

The properties of the velocity dispersion tensor is another puzzle. The velocity dispersion profile is slightly rising at small radii and slightly falling at large radii but is rather flat overall (Huss, Jain & Steinmetz 1999a; 1999b). The profile of the anisotropy parameter $\beta(r)$ indicates near isotropy at small radii that is developing gradually into more radial orbits at large radii (Colin et al. 2000). For a spherical system in equilibrium, the $\sigma(r)$ and $\beta(r)$ are related to $\rho(r)$ via the Jeans equation, but it is not at all clear why $\sigma(r)$ or $\beta(r)$ have these specific shapes.

An interesting attempt to address the origin of the halo profile has been made by Taylor & Navarro (2001), who measured a poor-man phase-space density profile by $f_{\text{TN}}(r) = \rho(r)/\sigma(r)^3$, and found that it displays an approximate power-law behavior, $f_{\text{TN}} \propto r^{-1.87}$, over more than two decades in r . Using the Jeans equation, they showed that this power law permits a whole family of density profiles, and that a limiting case of this family is a profile similar to NFW, but with an asymptotic slope of -0.75 as $r \rightarrow 0$. This scale-free behavior of $f_{\text{TN}}(r)$ is intriguing, and it motivates further studies of halo structure by means of phase-space density.

The simulations of the Λ CDM cosmology also reveal that the halos are built by a roughly self-similar hierarchical clustering process, where smaller building blocks accrete and merge into bigger halos. At every snapshot, every halo contains a substructure of subhalos on top of a smooth halo component that has been tidally stripped from an earlier generation of substructure. Some of the important dynamical processes involved in this hierarchical halo buildup are understood qualitatively, including dynamical friction, tidal stripping and mergers. However, a complete understanding of how these processes work in concert to produce the halo structure and kinematics is lacking.

Attempts have been made to explain an inner density cusp using toy models of dynamical stripping and tidal effects during the halo buildup by mergers (e.g. Syer & White 1998; Dekel, Devor & Hatzroni 2003; Dekel et al. 2003). However, a similar halo density profile seems to be produced also in simulations where substructure has been artificially suppressed (Moore et al. 1999b; Alvarez, Shapiro & Martel 2002), indicating that the process responsible for the origin of this density profile might be a more robust feature of gravity.

The issue of halo substructure has become timely both observationally and theoretically. Tidal streams associated with dwarf satellite galaxies are observed in the halos of the Milky Way and M31 and reveal their histories (Ibata et al. 2001; this proceedings). Gravitational-lenses provide preliminary indications for the presence of substructure in halos at the level predicted by the Λ CDM scenario (Dalal & Kochanek 2002). In contrast, the observed number density of dwarf galaxies seems to be significantly lower, thus posing a “missing dwarf problem” (Klypin et al. 1999; Moore et al. 1999a). Also, the “angular-momentum problem” of disk galaxies (e.g. Navarro & Steinmetz 2000; Bullock et al. 2001a)

is probably associated with the evolution of substructure in halos (Maller & Dekel 2002; Maller, Dekel & Somerville 2002). While these problems necessarily involve baryonic processes, understanding the gravitational evolution of substructure is clearly a prerequisite for solving them.

Aiming at the origin of halo structure, we report here on a first attempt by Arad, Dekel & Klypin (2004, ADK) to address directly the halo phase-space structure. The fundamental quantity in the dynamical evolution of gravitating systems is the full, 6D, phase-space density $f(\mathbf{x}, \mathbf{v})$, which intimately relates to the underlying Vlasov equation, and lies behind any (violent) relaxation process that gives rise to the virialized halo structure. Ideally, one would have liked to compute f free of assumptions regarding spherical symmetry, isotropy, or any kind of equilibrium, but computing densities in a 6D space is a non-trivial challenge. The state-of-the-art N-body simulations, with more than million particles per halo, allow for the first time an attempt of this sort. ADK developed a successful algorithm for measuring $f(\mathbf{x}, \mathbf{v})$, and studied its relevant properties and the associated systematic and random uncertainties. They then applied this algorithm to simulated virialized halos in the Λ CDM cosmology, and obtained two surprising new results. First, the phase-space volume distribution of f is a universal power-law, valid in all virialized halos that form by hierarchical clustering. Second, this power law is not directly related to the overall density profile, but is rather driven by the halo substructure. We thus learn that $f(\mathbf{x}, \mathbf{v})$ provides a useful tool for studying the hierarchical buildup of dark-matter halos and the evolution of substructure in them.

2. More about f and $v(f)$

A collisionless system is completely determined by the fine-grained phase-space density function $f(\mathbf{x}, \mathbf{v}, t)$. The evolution of f is governed by the Vlasov equation,

$$\partial_t f + \mathbf{v} \cdot \nabla_{\mathbf{x}} f - \nabla_{\mathbf{x}} \Phi \cdot \nabla_{\mathbf{v}} f = 0 , \quad (1)$$

with $\Phi(\mathbf{x})$ the gravitational potential, related self-consistently to $f(\mathbf{x}, \mathbf{v})$ by the Poisson's integral

$$\Phi(\mathbf{x}) = -G \int d\mathbf{x}' d\mathbf{v} \frac{f(\mathbf{x}', \mathbf{v})}{|\mathbf{x} - \mathbf{x}'|} . \quad (2)$$

We therefore assume that a true understanding of the nature of self-gravitating collisionless systems must involve $f(\mathbf{x}, \mathbf{v})$ as a primary ingredient.

While the 6D $f(\mathbf{x}, \mathbf{v})$ is hard to deal with, there is a simpler function, $v(f)$, which is intimately related to $f(\mathbf{x}, \mathbf{v})$, yet is much simpler to handle. It is defined as

$$v(f = f_0) \equiv \int d\mathbf{x} d\mathbf{v} \delta[f(\mathbf{x}, \mathbf{v}, t) - f_0] , \quad (3)$$

such that $v(f)df$ is the volume of phase-space occupied by phase-space elements whose density lies in the range $(f, f + df)$. The Vlasov equation ensures that every phase-space element preserves its density along its path, as therefore $v(f)$ is conserved.

However, as the system evolves, phase-space patches of high f are stretched and spiral into regions with low f , and become thinner such that f is varying

over increasingly smaller scales. At some point one can no longer measure f but rather an average of it over some finite volume, referred to as the “coarse-grained” phase-space density, which we denote \bar{f} . The coarse-grained $\bar{v}(\bar{f})$ is no longer conserved. In the course of a collapse or merger of a dark-matter halo, rapid global fluctuations of the gravitational potential re-distribute the energies of each phase-space element and lead to mixing. After a few global dynamical times, the potential fluctuations fade away, \bar{f} stabilizes, and it can be viewed as the “physical” phase-space density of the system, since the microscopic fluctuations of f can no longer be measured or affect the gravitational potential.

One obvious constraint on the final \bar{f} , as an average of f , is that their maximum values must obey $\bar{f}_{\max} \leq f_{\max}$. Since the initial $\bar{v}(\bar{f})$ is identical to $v(f)$, if the initial $\bar{v}(\bar{f})$ vanishes for $f > f_{\max}$, then so does the final $\bar{v}(\bar{f})$. There are several additional constraints imposed by the given $v(f)$ on the final $\bar{v}(\bar{f})$, specified by the *mixing theorem* (Tremaine, Hénon & Lynden-Bell 1986), whose strength is rather limited because it only provides an integro-differential inequality constraint on $\bar{v}(\bar{f})$.

In general, the same $v(f)$ can describe for different systems. However, if the system is spherically symmetric and stationary, such that f is a function of the energy alone, $f(\mathbf{x}, \mathbf{v}) = f(\epsilon)$, then there is a unique relation between $v(f)$, $f(\epsilon)$ and $\rho(r)$. In particular, using dimensional arguments and the virial theorem, one can show that if $\rho(r) \propto r^{-\alpha}$, then $v(f) \propto f^{-\beta}$ with

$$\alpha = \frac{18 - 6\beta}{4 - \beta} . \quad (4)$$

Therefore, the values in the range $0 \leq \alpha \leq 2$, which are relevant for the inner regions of halos where f is high, correspond to a narrow range of β values, $3 \geq \beta \geq 2.5$. The value $\beta = 2.5$ corresponds to the singular isothermal sphere $\alpha = 2$, while $\beta = 2.8$ corresponds to an $\alpha = 1$ cusp, and $\beta = 3$ corresponds to a flat core, $\alpha = 0$.

3. Measuring $v(f)$ in an N -body System

We wish to measure the 6D $f(\mathbf{x}, \mathbf{v})$ of a system represented by N particles of mass m each. Counting particles in uniform cells is impractical because even with 10^6 cells there would be only 10 cells along each axis. We therefore use an adaptive grid, where the cells vary in size and in shape to allow a proper resolution where needed. A particularly robust method of this type is based on the *Delaunay Tessellation* (Delaunay 1934), which has already been implemented in a cosmological context in 3D (Bernardeau & van de Weygaert 1996; Schaap & van de Weygaert 2000).

A tessellation is the division of R^d space into a complete covering of mutually disjoint convex polygons. In the Delaunay tessellation, every $d + 1$ points whose circumsphere [i.e., the $(d - 1)$ -dimensional sphere that passes through all of them] does not encompass any other point define a d -dimensional polyhedron which makes a *Delaunay Cell*. ADK followed van de Weygaert (1994) in using the algorithm by Tanemura, Ogawa & Ogita (1983). An analysis of a halo with 10^6 particles, which lasts about a week on a standard CPU, produces $\sim 10^9$ cells. A

typical particle is surrounded by $\sim 7,000$ cells, made out of ~ 200 neighboring particles.

The value of f at particle i is estimated by $f_i \equiv (d+1)m/V_i$, where V_i is the total volume of all the cells neighboring to particle i , d is the dimensionality (here $d = 6$), and the factor $d+1$ ensures mass conservation. In order to estimate f at any point (\mathbf{x}, \mathbf{v}) , one averages over the f_i 's of the seven particles that define the cell. The desired $v(f)$ is obtained by first computing its cumulative version $V(f)$,

$$V(f_0) = \int_{f_0}^{\infty} v(f') df' = \int_{f(\mathbf{x}, \mathbf{v}) > f_0} d\mathbf{x} d\mathbf{v} \rightarrow \sum_{f_\nu > f_0} |D_\nu|, \quad (5)$$

and then differentiating $v(f) = -dV(f)/df$. The sum in the above formula is of all volumes of Delaunay cells D_ν , whose average f_ν is greater than f_0 . In what follows, we sometimes denote the Delaunay-measured f and $v(f)$ by f_{del} and v_{del} .

When measuring the $v(f)$ of a cosmological N -body system, one expects two types of errors. First, the errors in the underlying f associated with errors in the numerical simulation itself, e.g., due to two-body relaxation effects, force estimation, or time integration. A way to estimate these errors is by re-simulating the same system with different codes and with different sets of numerical parameters. A systematic testing of this sort will be reported elsewhere (Arad, Dekel & Stoehr, in prep.). Meanwhile, ADK compared several different halos simulated with different resolutions and with different codes, and found that all the halos tested recover almost the same $v(f)$.

The other type of errors originate from the fact that we estimate a smooth f from a finite set of particles using a specific adaptive technique. Here one may encounter both statistical and systematic errors. Some of these errors would decrease as the number of particles is increased, whereas other errors are an inherent part of the method. ADK introduced a simple statistical model based on Varonoi tessellation, which resembles the Delaunay technique and yet lends itself more easily to analytical treatment. The predictions of this model were then tested against numerical experiments with synthetic systems.

It is found that f_{del} at each particle is drawn from a probability distribution function of $f_{\text{del}}/f_{\text{true}}$. In a typical realization with 10^6 particles, the width of this distribution is about one decade, describing the typical fluctuations of f_{del} about f_{true} . As the number of particles $N \rightarrow \infty$, the shape of the distribution approaches an asymptotic limit, with a *finite* width of about one quarter of a decade, implying local fluctuations even in the infinite limit.

It is then realized that $v_{\text{del}}(f)$ can be viewed as a convolution of the true $v(f)$ and a fixed window function,

$$v_{\text{del}}(f = f_0) = \int_0^{\infty} v_{\text{true}}(f) f_0^{-1} p(f_0/f) df. \quad (6)$$

If $v(f)$ is close to a power-law, the difference between $v_{\text{del}}(f)$ and $v_{\text{true}}(f)$ is negligible over a large range of scales. This is a very useful feature of the method.

The relative statistical error in $v_{\text{del}}(f)$ is proportional to $1/\sqrt{N}$, and can be approximated by

$$\Delta f \simeq \left(\frac{m}{f \langle V_{\text{del}}(f) \rangle} \right)^{1/2}, \quad (7)$$

with $V_{\text{del}}(f) = \int_f^\infty v_{\text{del}}(f') df'$ and $m = M/N$. In practice, this means that when $N \geq 10^6$, the statistical error is negligible for a very wide range of f . Moreover, in regions where there are large statistical errors, these errors are usually overwhelmed by systematic errors.

4. A Universal Scale-Free $v(f)$

The $v(f)$ is measured from several different halos, in three different mass ranges, simulated within the Λ CDM cosmology with two different N -body codes. We focus on virialized halos out to slightly outside the virial radius. The value of f that can be crudely associated with the virial radius of a given halo, where one may expect a qualitative change in the behaviour of $v(f)$, is estimated by $f_{\text{vir}} = \pi^{-3/2} \rho / \sigma^3$, with ρ and σ the mean virial quantities. On the other side, the reliable-measurement range is marked by $f = f_{20\%}$, below which the statistical error in $v(f)$ due to the DTFE is below 20% according to eq. 7. This formula was verified by the $v(f)$ of mock systems with 10^5 particles. The statistical error is expected to be practically negligible in the range $f_{\text{vir}} < f < f_{20\%}$. When tested using synthetic datasets for which the true $v(f)$ is known, we learn that with 10^5 particles the method recovers the true $v(f)$ very well over a range of 5-6 decades in f , while with 10^6 particles the range spans ~ 10 decades.

The results described in ADK are based on three different cosmological simulations, two using the ART code (Kravtsov, Klypin & Khokhlov 1997), and the third using the TPM code (Bode, Ostriker & Xu 2000; Bode & Ostriker 2003). The assumed cosmological model is the standard Λ CDM with $\Omega_m = 0.3$, $\Omega_\Lambda = 0.7$ and $h = 0.7$ today. Halos were sampled from the simulated periodic boxes of sides $L = 1, 25$ and $320 h^{-1} \text{Mpc}$, which we denote $L1$, $L25$ and $L320$. The simulations are by Colin et al. (2003), by Klypin et al. (2001), and by Wambsganss, Bode & Ostriker (2004) and Weller, Bode & Ostriker (2004). The force resolution is 87, 140 and 4700pc. The particle mass is 7×10^3 , 1.2×10^6 and $2.6 \times 10^9 M_\odot$. The halo masses analyzed from these simulations correspond to dwarf galaxies ($10^9 - 10^{10} M_\odot$), normal galaxies ($\sim 10^{12} M_\odot$) and clusters of galaxies ($\sim 10^{15} M_\odot$) respectively. The ART halos were sampled by $\sim 10^6$ particles within $\sim 1.1 R_{\text{vir}}$, while the TPM halos were sampled by only 4×10^5 particles within the corresponding radius. The L1 halos were analyzed at $z = 2.33$. More details about the simulations and the halo properties are summarized in Table 1 of ADK. The $v(f)$ curves for these nine halos are shown in Fig. 1

The figure shows that in every halo $v(f)$ is well fit by a power-law,

$$v(f) \propto f^{-2.50 \pm 0.05}, \quad (8)$$

over 3 to 5 decades in f . It is typically valid between about f_{vir} and slightly below $f_{20\%}$. Outside this range, $v(f)$ gradually deviates downward. In the low- f regime the deviation is associated with departure from the virial regime, while

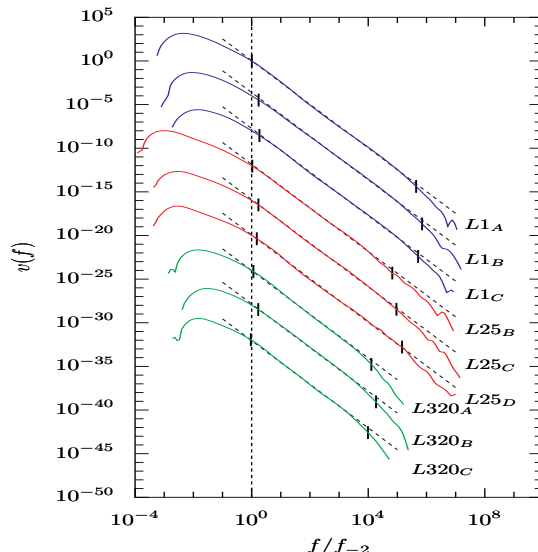


Figure 1. The volume distribution of phase-space density, $v(f)$, for each of the nine halos analysed in ADK. The curves were shifted to coincide at $f = f_{-2}$, where the local log slope of $v(f)$ is -2 , and were then shifted vertically by 4 decades relative to each other. A power-law line $v(f) \propto f^{-2.5}$ is shown on top of each curve. Marked on each curve are the virial-radius level f_{vir} and the 20% statistical error limit $f_{20\%}$.

the high- f deviation is consistent with being due to the limited mass resolution, as indicated by $f_{20\%}$ and by the error analysis of ADK. The high- f deviation from the power-law tends to occur at a smaller f value in L25, and even smaller in L320, due to the fact that M_{vir} is smaller respectively.

The power law in $v(f)$ does not show a significant dependence on halo mass. There may be a marginal trend for slight steepening of $v(f)$ as a function of mass, but only from steeper than $f^{-2.45}$ at $\sim 10^9 M_{\odot}$ to flatter than $f^{-2.55}$ at $\sim 10^{15} M_{\odot}$. This indicates relative insensitivity to the exact slope of the initial fluctuation power spectrum, which varies across the range from dwarf galaxies to clusters of galaxies. Additionally, the fact that we obtained essentially the same $v(f)$ from simulations using two different numerical codes, indicates that the shape of $v(f)$ is not an artifact of a particular simulation technique.

5. Substructure

When $f(\mathbf{x}, \mathbf{v})$ is function of the energy alone, and the halo is spherical and isotropic, the power-law $v(f) \propto f^{-2.5}$ implies via eq. 4 that the real-space density profile must also be a power law, in fact an isothermal sphere $\rho(r) \propto r^{-2}$, at least over some finite range in r . This is clearly not the case (§1), indicating that f is not a function of energy alone, and the system must deviate from spherical symmetry or isotropy. This could be due to the clumpy substructure of the halo, where the surviving subhalos contribute high phase-space densities to $v(f)$, thus

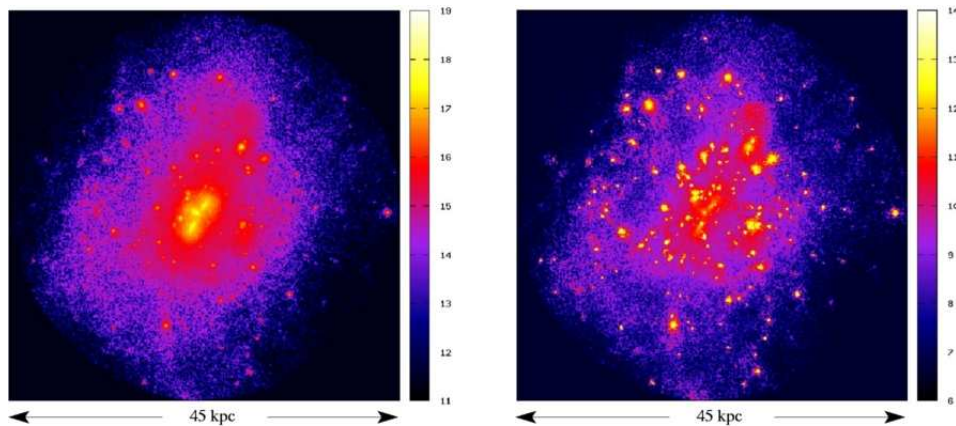


Figure 2. Density maps of dwarf halo $L1_B$ in a slice of thickness $0.4R_{\text{vir}}$. Left: real-space density. Right: phase-space density. The units in the colour key are $\log(\rho/[M_{\odot} \text{Mpc}^{-3}])$ and $\log(f/[M_{\odot} \text{Mpc}^{-3} \text{km}^{-3} \text{s}^3])$ respectively. The very-high f values are found inside clumps which are typically far away from the halo center.

making it shallower than expected from a smooth system with an inner density slope flatter than -2 .

Figure 2 shows density and phase-space density maps of an equatorial slice from one of the halos, in which the color represents the densities ρ and f averaged over the values assigned to each particle in a small real-space volume (of side $\sim 0.005R_{\text{vir}}$). The ρ of each particle was calculated using a 3D Voronoi tessellation (van de Weygaert 1994), which is similar in its adaptive nature to the Delaunay tessellation used to estimate f . While the real-space density maps are dominated by the familiar smooth trend of density decreasing outward, perturbed by several tight clumps throughout the halo, the global trend with radius becomes much less prominent in the phase-space density maps, with the subhaloes contributing the highest peaks, especially in the outer regions of the halo. Moderate f peaks are found everywhere (reddish yellow), and the very high peaks (bright yellow) are preferentially found in the periphery. The central peak in f is quite modest in comparison; the elongated structures near the center of the halo are most likely merging subhalos.

Figure 3 shows ρ and f associated with a random subset of the N-body particles as a function of their distance r from the halo center. A large portion of these particles follow the global trend of decreasing density with radius – they could be associated with a smooth-background component, for which f is approximately a function of energy alone. At radii $r > 1$ kpc, the high- f values come in as “spikes” corresponding to the subhalos. While the spikes in ρ reach values comparable to the central peak, the spikes in f could be more than 100 times higher, indicating that the subhalos are both *compact* and *cold*.

The spikes seem to be lower and broader as they get closer to the halo center, and they completely blend into the smooth background inside ~ 2 kpc. This indicates that the subhalos phase-mix and lose their high phase-space densities

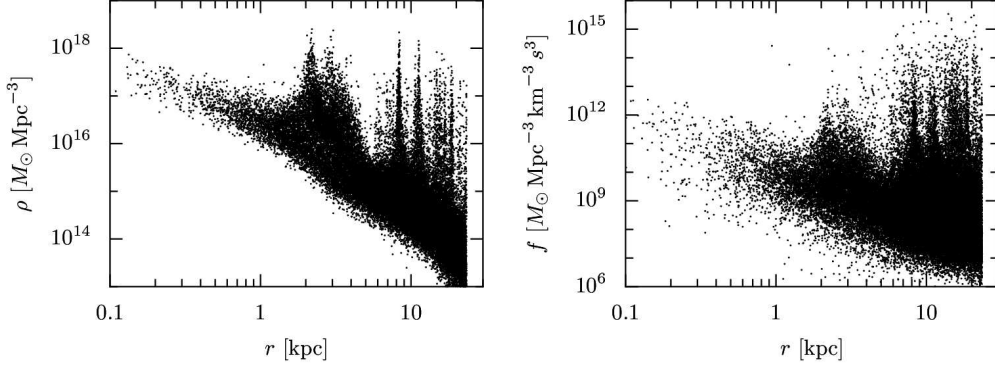


Figure 3. Densities as a function of radius for dwarf halo $L1_B$, using a random set of 4% of the particles. Left: real-space density. Right: phase-space density. The background particles define a general trend of decreasing density with radius, while the spikes correspond to subhalos. The phase-space density spikes are higher than the central peak because the subhalos are cold. They become shorter and broader at smaller radii, indicating heating by tidal effects and mergers.

as they approach the halo center. This seems to be the natural result of mergers and *tidal effects*, which puff up the subhaloes and especially heat them up.

As a first attempt at trying to understand how the power law $v(f) \propto f^{-2.5}$ in a halo of mass M may originate from its substructure, one may simply add up the typical contributions from the general population of halos of different masses m smaller than M , as predicted in the Λ CDM cosmology. Based on cosmological N-body simulations (e.g., Moore et al. 1999a; Ghinga et al. 2000; De Lucia et al. 2004), and in accordance with the Press-Schechter (1974) approximation, the mass function of small-mass halos can be approximated by $dn/dm \propto m^{-\gamma}$, with $\gamma \simeq 1.8 - 2.0$. Supported by the simulations, one assumes that the average density profiles of halos of different masses are simply scaled versions of each other (e.g., Navarro et al. 1996). If all the halos form at the same time, they have the same characteristic real-space density $\rho_m = \rho$, so their typical radii scale like $r_m \propto m^{1/3}$. Based on the virial theorem, the velocity dispersions then scale like $\sigma_m \propto m^{1/3}$. Therefore, the typical phase-space volume of a halo of mass m scales like $V_m \propto r_m^3 \sigma_m^3 \propto m^2$, and its typical phase-space density is $f_m \propto m/V_m \propto m^{-1}$. With this scaling one can show that $v(f)$ should be flatter than $v(f) \propto f^{-(4-\gamma)}$. For $\gamma \geq 1.8$, this means that $v(f)$ is shallower than $f^{-2.2}$, which is significantly shallower than the measured $f^{-2.5 \pm 0.05}$. Including the fact that small halos form first in a Λ CDM scenario makes a negligible difference. One can conclude that the population of subhalos within a bigger host halo must be different than the general population of halos. As a result of mergers and tidal effects, the subhalos are expected to have a different mass function, their shape properties are likely to vary differently with mass, and both effects probably vary with radius. Thus, the phase-space density is likely to provide a useful tool for studying the dynamical evolution of subhalos in their parent halos.

6. Discussion

It is important to verify that these results are not numerical artifacts. Based on the error analysis and tests with mock datasets, we believe that the $v(f)$ measured by the DTFE algorithm genuinely reflects the true phase-space properties of the given N -body system over a broad range of f . The question is whether the phase mixing suffered by the subclumps is an artifact of numerical effects such as few-body relaxation, leading to underestimated inner densities and/or overestimated internal velocities (Binney 2003). The apparent agreement between simulations run with different codes and different resolutions is encouraging. In order to specifically address the effect of two-body relaxation, we intend to run twice a simulation of the same halo with the same number of particles but with a different force resolution (ongoing work with F. Stoehr).

Assuming that the simulations genuinely reflect the true physical behaviour, the origin of the robust power-law shape of $v(f)$ from the merging substructure becomes a very interesting theoretical issue. As demonstrated in §5, a simple model using the mass function and the scaled profiles of the general halo population in the Λ CDM scenario does not reproduce the correct power law. This, and the apparent trend of the f spikes with radius, indicate that the structural and kinematical evolution of the subhaloes in the parent halo are important. Studies of tidal heating and stripping may be found useful in this modelling.

It would be interesting to follow the phase-space evolution and the contribution to the overall $v(f)$ by a single, highly resolved subhalo, or many of those, as they orbit within the parent halo and approach its center. This may help us understand the nature of the interaction between the parent halo and its subhaloes, and the origin of the $v(f)$ power law (ongoing works with E. Hayashi and with B. Moore).

We saw that the power-law behavior of $v(f)$ is limited to the virial regime. It would be interesting to learn how this shape evolves in time as the halo virializes. A preliminary study (to be concluded and reported in another paper) indicates that in the intermediate- f regime the $v(f)$ of a pre-virialized system is significantly flatter than $f^{-2.5}$, while in the high- f regime it drops in a much steeper way. The $f^{-2.5}$ behavior seems to be a feature unique to virialized systems.

We learned that in the haloes that are built by hierarchical clustering, the power-law behavior $v(f) \propto f^{-2.5}$ reflects the halo substructure. It would be interesting to find out whether this power-law behavior actually requires substructure, or it is a more general phenomenon of virialized gravitating systems, valid independently of substructure. One way to answer this question would be to analyse simulated haloes in which all fluctuations of wavelengths smaller than the halo scale were removed, resulting in a smooth halo formed by monolithic collapse, with no apparent substructure in the final configuration. As described in §1, such haloes are known to still have NFW-like density profiles in real space, and one wonders whether they also have the magic power-law $v(f)$. There are preliminary indications for a steeper $v(f)$ in this case (Arad, Dekel & Moore, in preparation). If confirmed, it would indicate that the $f^{-2.5}$ behavior, while insensitive to the exact slope of the initial power spectrum, is unique to the hierarchical clustering process, and is not a general result of violent relaxation.

Our current results are just first hints from what seems to be a promising rich new tool for analysing the dynamics and structure of virialized gravitating systems. The analysis could become even more interesting when applied to haloes including the associated gaseous and stellar components.

Acknowledgments. We thank Paul Bode, Stefan Gottloeber, Eric Hayashi, Anatoly Klypin, Ben Moore, Julio Navarro and Felix Stoehr for their ongoing collaborations on the various parts of this projet. We acknowledge stimulating discussions with Stefan Colombi, Donald Lynden-Bell, Gary Mamon, Jerry Ostriker and Simon White. IA is a Marie Currie Fellow. AD is a Miller Visiting Professor at UC Berkeley. This research has been supported by the Israel Science Foundation grant 213/02, by the German-Israel Science Foundation grant I-629-62.14/1999, and by NASA ATP grant NAG5-8218.

References

- Alvarez M.A., Shapiro P.R., Martel H., 2002, AAS, 200, 4103
 Arad I., Dekel A., Klypin A.A., 2004, MNRAS, submitted, astro-ph/0403106 (ADK).
 Bernardeau F., van de Weygaert R., 1996, MNRAS, 279, 693
 Binney J., 2003, MNRAS, astro-ph/0311155
 Bode P., Ostriker J.P., Xu G., 2000, ApJS, 128, 561
 Bode P., Ostriker J.P., 2003, ApJS, 141, 1
 Bullock J.S., Dekel A., Kolatt T.S., Kravtsov A.V., Klypin A.A., Porciani C., Primack J.R., 2001a, ApJ, 555, 240
 Bullock J.S., Kolatt T.S., Sigad Y., Somerville R.S., Kravtsov A.V., Klypin A.A., Primack J.R., Dekel A., 2001b, MNRAS, 321, 559
 Colín P., Klypin A.A., Kravtsov A.V., 2000, ApJ, 539, 561
 Colín P., Klypin A.A., Valenzuela O., Gottlöber S., 2003, ApJ, submitted, astro-ph/0308348
 Dalal N., Kochanek C.S., 2002, ApJ, 572, 25
 Dekel A., Devor J., Hetzroni, G., 2003, MNRAS, 341, 326.
 Dekel, A., Arad, I., Devor, J., Birnboim, Y., 2003, ApJ, 588, 680
 Delaunay B. V., 1934, Bull. Acad. Sci (VII) Classe Sci. Mat., 793
 De Lucia G., Kauffmann G., Springel V., White S.D.M., Lanzoni B., Stoehr F., Tormen G., Yoshida N, 2004, MNRAS, 348, 333
 Ghigna S., Moore B., Governato F., Lake G., Quinn T., Stadel J., 2000, ApJ, 544, 616
 Hayashi E., Navarro J.F., Power C., Jenkins A., Frenk C.S., White D.M., Springel V., Stadel J., Quinn T.R., MNRAS, submitted, astro-ph/0310576
 Huss A., Jain B., Steinmetz M., 1999a, ApJ, 517, 64
 Huss A., Jain B., Steinmetz M., 1999b, MNRAS, 308, 1011
 Ibata R., Irwin M., Lewis G.F., Stolte A., 2001, ApJ, 547, 133
 Lynden-Bell D., 1967, MNRAS, 136, 101
 Klypin A.A., Kravtsov A.V., Valenzuela O., Prada, F., 1999, ApJ, 522, 82

- Klypin A.A., Kravtsov A.V., Bullock J.S., Primack J.R., 2001, *ApJ*, 544, 903
- Kravtsov A.V., Klypin A.A., Khokhlov A.M., 1997, *ApJS*, 111, 73
- Maller A.H., Dekel A., 2002, *MNRAS*, 335, 487
- Maller A.H., Dekel A., Somerville, R.S., 2002, *MNRAS*, 329, 423
- Moore B., Ghigna S., Governato F., Lake G., Quinn T., Stadel J., Tozzi P., 1999a, *ApJ*, 524, L19
- Moore B., Quinn T., Governato F., Stadel J., Lake, G., 1999b, *MNRAS*, 310, 1147
- Navarro J.F., Frenk C.S., White S.D.M., 1996, *ApJ*, 462, 563
- Navarro J.F., Frenk C.S., White S.D.M., 1997, *ApJ*, 490, 493
- Navarro J.F., Steinmetz M., 2000, *ApJ*, 538, 477
- Navarro J.F., Hayashi E., Power C., Jenkins A., Frenk C.S., White S.D.M., Springel V., Stadel J., Quinn T.R., *MNRAS*, submitted, astro-ph/0311231
- Power C., Navarro J.F., Jenkins A., Frenk C.S., White, S.D.M., Springel V., Stadel J., Quinn T.R., *MNRAS*, 338, 14
- Press W.H., Schechter P., 1974, *ApJ*, 187, 425
- Schaap, W., van de Weygaert R., 2000, *A&A*, 363, L29
- Syer D., White S.D.M., 1998, *MNRAS*, 293, 337
- Tanemura M., Ogawa T., Ogita N., 1983, *Journal of Computational Physics*, 51, 191
- Taylor J.E., Navarro J.F., 2001, *ApJ*, 563, 483
- Tremaine S., Hénon M., Lynden-Bell D., 1986, *MNRAS*, 219, 285
- van de Weygaert R., 2000, *A&A*, 363, L29.
- Wambsganss J., Bode P., Ostriker J.P., *ApJ*, submitted, astro-ph/0306088
- Weller J., Bode P., Ostriker, J.P., in preperation.